NUMATRON and TARN

T. Katayama, A. Noda and Y. Hirao

Institute for Nuclear Study, University of Tokyo,
Tokyo, JAPAN

ABSTRACT

General descriptions of the NUMATRON design and related technical developments at INS, University of Tokyo, are reported. A test accumulation ring for NUMATRON project, TARN, was constructed for integrating various technical developments. Recent results of injection test using this ring are also described.

1. INTRODUCTION

In recent years, interests in high-energy heavy-ions have been growing up not only in the field of nuclear physics but also in the fields of atomic physics, solid-state physics, medical biology, fusion power generation engineering and many other sciences and applications. In Japan, an accelerator complex has been proposed at INS, University of Tokyo, which is named NUMATRON[1,2] and should provide heavy ions up to uranium in an energy range of 0.1 ∿ 1.3 GeV per nucleon. After completion of detailed design of the NUMATRON the major activity of the study group has been directed to the construction of the test accumulation ring for NUMATRON, TARN, which is a test facility not only for studying multiturn injection and RF stacking but also for integrating various technical developments.

In following sections, the outline of the NUMATRON is described as well as that of the TARN and preliminary results of the beam injection.

2. GENERAL DESIGN OF NUMATRON

The proposed accelerator consists of Cockcroft-Walton generators, three Wideröe linacs, two Alvarez linacs and two synchrotrons (Fig.1).

Two identical preaccelerators are arranged symmetrically in order to be able to operate in parallel. Each preaccelerator has a 500 kV high voltage generator and two ion source terminals. The acceleration voltage is adjustable in a wide range so that ions of various charge-to-mass ratios can be accelerated to a constant velocity. After passing through the buncher section, ions are injected into a row of three Wideröe linacs of a resonant frequency of 25 MHz. The first and the second are operated in π-3π mode and the third in π-π mode. The last Wideröe linac is followed by an Alvarez linac with a resonant frequency of 100 MHz at the energy of 1 MeV/u. Two stripper sections with achromatic charge analyzing systems are installed at the specific energies of 0.3 and 1.6 MeV/u in order to obtain an efficient acceleration. The injector linac specifications are shown in Table 1.

Table 1 The Injector Linac Specifications

	Wideröe 1	Wideröe 2	Wideröe 3	Alvarez 1	Alvarez 2
Operation Mode	π-3π, 38 gaps	π-3π, 20 gaps	π-π, 36 gaps	2π, 46 gaps	2π, 108 gaps
Synchrotron Phase (deg.)	-30.0	-30.0	-30.0	-25.84	-25.84
T/A (MeV/u)	0.015 - 0.146	0.146 - 0.305	0.305 - 1.102	1.120 - 1.603	1.600 - 10.023
v_j/c (%)	0.562 - 1.768	1.768 - 2.557	2.557 - 4.861	4.861 - 5.859	5.854 - 14.553
ε	0.0294 (U^{7+})	0.0294 (U^{7+})	0.0672 (U^{16+})	0.0672 (U^{16+})	0.193 (U^{46+})
L (m)	5.5	5.4	8.0	7.5	32.1
$\Delta T/(L\cdot\varepsilon)$ (MeV/m)	0.85	1.00	1.49	0.988	1.36
Z_{eff} (MΩ/m)	67.8	36.0	47.6	41.8 - 43.4	43.3 - 31.6
Power Loss (MW)	0.076	0.215	0.494	0.206	1.903
Q-magnet Sequence	FDFD	FDFD	FFDD	FFDD	FFDD
G (kG/cm)	10.0 - 3.18	3.18 - 2.20	3.50 - 1.83	4.00 - 3.30	3.30 - 1.33
cosμ	0.849	0.849	0.572	0.906	0.906
Aperture (mmϕ)	20, 25, 30	30	35	40	40
Admittance (mm mrad)	114 π	88.7 π	127 π	248 π	203 π

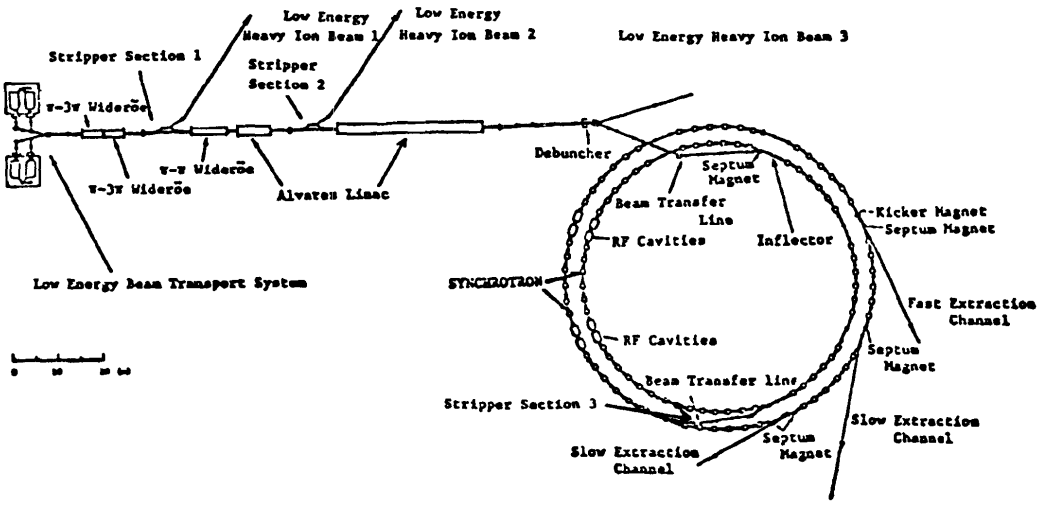

Fig. 1 Layout of NUMATRON

Final stage of the accelerator complex is composed of two synchrotrons. The first synchrotron has a capability of beam accumulation for obtaining heavy ions of high intensity. A combination of multiturn injection and RF stacking methods is applied to the injection scheme of the first ring.[3] The beam is accelerated up to the energy of 250 MeV/u and is extracted by a one turn ejection method. After passing through the final stripper section in the beam transport line between the first and the second synchrotrons, ions are completely stripped and injected into the second ring, where uranium ions are accelerated up to the maximum energy of 1270 MeV/u. The transition energy of the second synchrotron is 4.33 GeV and no ions are accelerated through the transition energy. The operation scheme of the linac and two synchrotrons is illustrated in Fig.2.

The RF systems in the rings are of two types, one of which is for RF stacking and the other is to accelerate the beams to the extraction energies. The former is described in the following Section on TARN.

The RF system for beam acceleration is designed so that the sweep range of frequency in the first ring is 1.65 $\sim$ 6.97 MHz, and in the second ring it is 3.6 $\sim$ 11.2 MHz for the various operation energies of the first and second synchrotrons. In the present design the magnetic fields of both synchrotrons vary linearly with time as $\dot{B}$ = 47.0 kG. s^{-1}, and then the

required RF peak voltage is around 20 kV for the synchronous phase angle of 30°. On the other hand, the energy spread of the accumulated beam in the first ring is 200 keV for the stacked number of 50, and the required peak RF voltage is determined so that the separatrix well covers the energy spread of the beam, namely 80 kV.

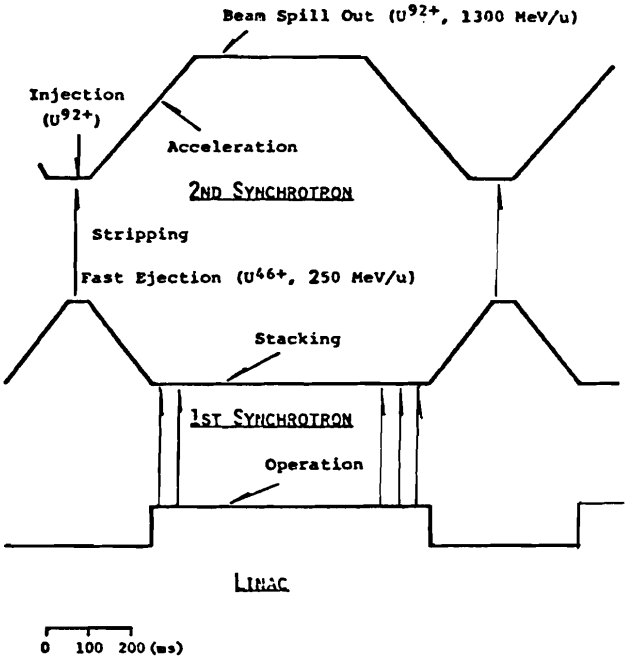

Fig.2 Operation Scheme of the Accelerator Complex

The required vacuum in the first ring is 2×10^{-11} torr for a survival rate of 90 % after an injection period of 1 sec, whereas in the second ring, 1×10^{-9} torr suffices to achieve the above survival rate because of its high energy operation. The output intensity of uranium is typically estimated at 10^9 particles per second, whereas for ions lighter than $Z \simeq 20$, it may be 10^{11} particles per second, limited by space charge effects.

In the present proposal, one fast ejection channel and two slow ejection channels are provided to answer the various needs for high energy heavy ion beams. Even at the final stage of the acceleration, the beam size is rather large and it is important that the ejection system is safe against beam blow up. From this point of view, we adopt the third integer resonance, although in this extraction mode, the arrangements of non-linear magnets will largely affect the emittance, spill time and the size of stable region.

The main parameters of the accelerator complex are given in Table 2.

Table 2 Numatron Parameters

A. Particle, Energy and Intensity

Particle	Max. Energy (GeV/u)	Intensity (pps)
U^{92+}	1.27	$\sim 10^{9}$
Kr^{36+}	1.47	$\sim 10^{11}$*
Ne^{10+}	1.81	$\sim 10^{11}$*

*Space Charge Limit

B. Injector	T/A(MeV)	Freq. (MHz)	β(v/c)	ε(q/A)
Cockcroft-Walton (500 KV)	0.0147	—	0.006	0.029(U^{7+})
Widerӧe (π-3π)	0.146	25	0.018	—
Widerӧe (π-3π)	0.305	25	0.026	—
Stripping	—	—	—	0.067(U^{16+})
Widerӧe (π)	1.10	25	0.048	—
Alvarez	1.60	100	0.059	—
Stripping	—	—	—	0.193(U^{46+})
Alvarez	10.0	100	0.146	—

C. 1st Synchrotron

Injection Energy		10 MeV/u
Maximum Energy		250 MeV/u
Repetition Rate of RF Stacking		100
Momentum Spread of Stacked Beam		± 0.7 %
Useful Aperture	radial	18 cm
	vertical	5 cm
Vacuum		2×10^{-11} torr
Space Charge Limit		
Number of Particles/sec		

D. 2nd Synchrotron

Guide Field (B_{max})		18.0 kG
Quadrupole Field $(dB/dr)_{max}$		1.38 kG/cm
Repetition Rate		1 Hz
Magnetic Radius		9.55 m
Average Radius		33.6 m
Circumference		211.2 m
Number of Normal Periods		24
Number of Long Straight Sections		8
Focusing Structure		FODO
Useful Aperture	radial	9 cm
	vertical	3.5 cm
Number of Betatron Oscillations		6.25
Phase Advance per Normal Period		70°
Vacuum		1×10^{-9} torr

3. TEST ACCUMULATION RING FOR NUMATRON PROJECT — TARN —

The test Accumulation Ring for NUMATRON, TARN, is constructed for developing technical subjects related to the heavy ion accelerator complex. The heavy ion beams, for example N^{5+} of 8.5 MeV/u, from the INS-SF Cyclotron[4] are injected and accumulated in the TARN, as shown in Fig.3.

The main parameters of the TARN are given in Table 3. The ring consists of eight bending magnets and sixteen quadrupole magnets with a lattice structure of FODO type. The mean radius is 5.06 m and the bending radius of the central orbit is 1.333 m. The overall ring view is shown in Fig.4. The heavy ion beam is accumulated in the ring by a combination of multiturn injection and RF stacking method. Expected intensity of accumulated ions such as N^{5+} is 10^{10} particles. The lifetime of the stacked beam is determined mainly by the charge exchange reactions between heavy ions and residual gas molecules. Assuming the cross section of these reactions to be $\sim 3\times10^{-17}$ cm^2, the required pressure in the ring is 1×10^{-10} torr for a survival rate of 90% during a stacking time of 1 sec. In following Sections, the design and performance of the ring are described.

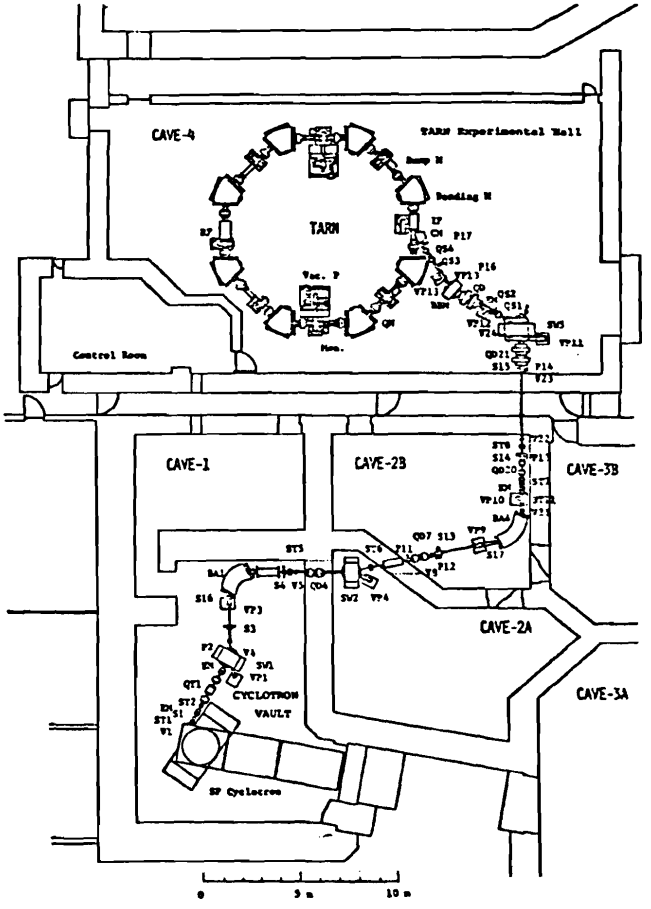

Fig.3 Layout of the TARN and the beam transport system from the SF Cyclotron. BA : Analyzer magnet. BBM : Bending magnet. SW : Switching magnet. Q : Quadrupole magnet. ST : Steering magnet. KM : Kicker magnet. S : Slit system. EM : Emittance monitor. P : Profile monitor. VP : Pumping system.

Table 3. Parameter List of the TARN

General		
Beam energy (for N^{5+})		8.56 MeV/u
Magnetic field		$B = 8.574$ kG
Bending radius		$\rho = 1.333$ m
Mean orbit radius		$R = 5.06$ m
Revolution frequency		$f_o = 1.259$ MHz
Betatron ν values		$\nu_x = 2.250$
		$\nu_y = 2.200$
Vacuum pressure		1×10^{-10} torr
Injection scheme		Multiturn injection
Magnet and Lattice		
Number of normal cells		8
Number of superperiods		8
Number of long straight sections		8
Periodic structure		Q_F B Q_D $\bar{O}$
Bending magnets		
Number		8
Gap		70 mm
Pole width		258 mm
Good field aperture		40×170 mm^2
Quadrupole magnets		
Number		16
Length		0.20 m
Field gradient		$k_F \simeq 0.240$ kG/cm
		$k_D \simeq 0.435$ kG/cm
Momentum compaction factor		Maximum = 1.70 m
		Minimum = 1.01 m
		Average = 1.41 m
Betatron amplitude function	(x)	(y)
	Maximum = 4.94 m	5.51 m
	Minimum = 1.08 m	1.18 m
RF Stacking System		
Frequency		8.81 MHz
Harmonic number		7
Maximum accelerating voltage		1.1 kV
Number of cavities		1
Total RF power		1.3 kW
Stacking parameter		
Momentum spread of the stacked beam		2.469 %
Momentum difference between the injection orbit and stack top		6.289 %
Repetition rate		50 Hz
Maximum RF stacking number		100

3.1 Magnetic Focusing System

The focusing structure of the TARN is a separated function FODO type, where both the superperiodicity and the number of normal cells are eight. The mean radius and the circumference of the ring are 5.06 m and 31.795 m, respectively, determined by considering the synchronization between the RF system of the TARN with a harmonic number of seven and that of the injector cyclotron. The number of betatron oscillations per revolution is around 2.25 both in horizontal and vertical directions. In Fig. 5, the working lines of the TARN for various sextupole corrections are shown.

(a)

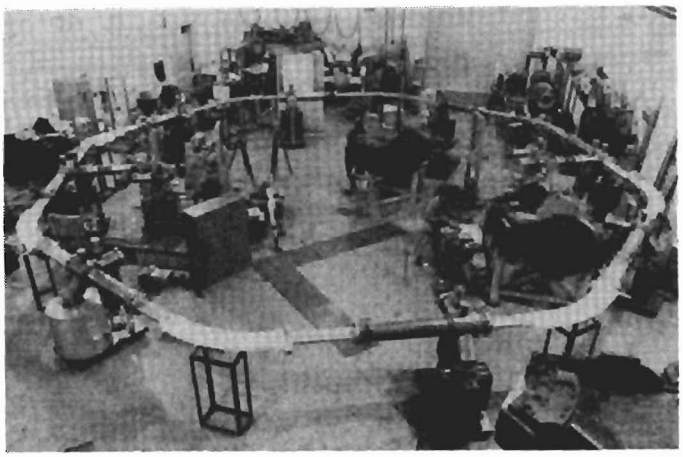

(b)

Fig. 4 a) Total view of the TARN. b) Vacuum system, arranged tentatively before the installation into the magnet gaps.

The useful aperture in the horizontal direction for the stacked beam is determined as 85 mm half width both in the bending magnet and qudrupole magnet, taking betatron oscillation amplitude, closed orbit displacement and the spread of closed orbit due to momentum spread of the stacked beam into account. The aperture of the bending magnet is 70 (height) x 258 (width) mm^2

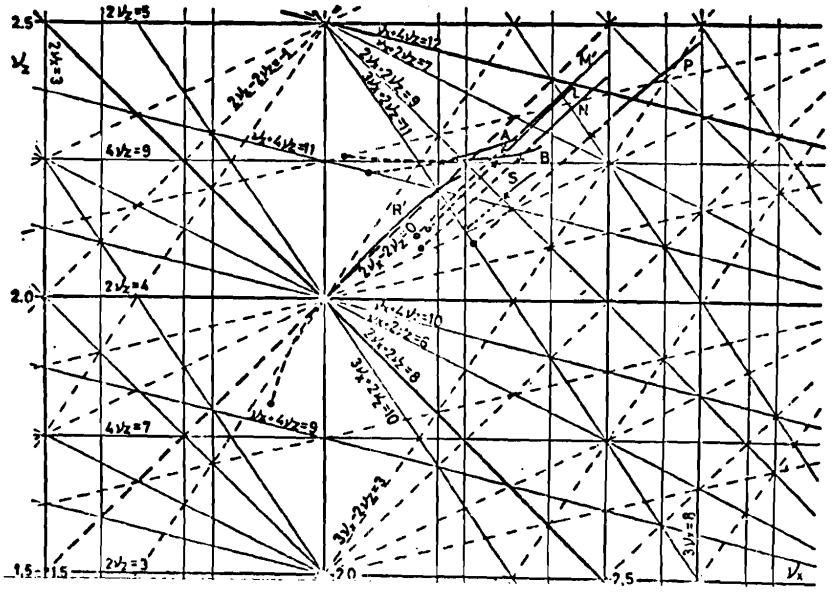

Fig.5 The work lines of the TARN. A and B represent the cases of the ideal and real magnets systems, respectively. Other lines (L ∿ R') represent the work lines with corrections.

including the thickness of the vacuum chamber wall, 4 mm, and spaces for heat insulation elements and distributed ion pumps. The radius of the inscribed circle of the quadrupole magnet is 65 mm.

The bending magnet is a window-frame type, which has merits of compactness of the structure and good field uniformity. In order to avoid the sagitta due to the small radius of curvature, 1.333 m, the magnet is fan-shaped. The edges of the magnet pole at both ends were designed to be normal to the central orbit. In order to reduce the flux density at the edge of the iron yoke, the pole edges were cut with four steps approximating Rogowski's curve. The shielding plates were attached at both ends considering the small distance between the bending magnet and quadrupole magnets. The shape of fringing field is shown in Fig.6.

The uniformity of the bending field along the radial direction was measured at the inner side of the magnet gap, sufficiently close to the edge, and was better than $\pm 2 \times 10^{-4}$ over the whole useful aperture.

The quadrupole magnet was designed to afford the possibility of AC operation to allow fast tuning of ν-values. The shape of the pole was determined using the computer program TRIM and is a hyperbola

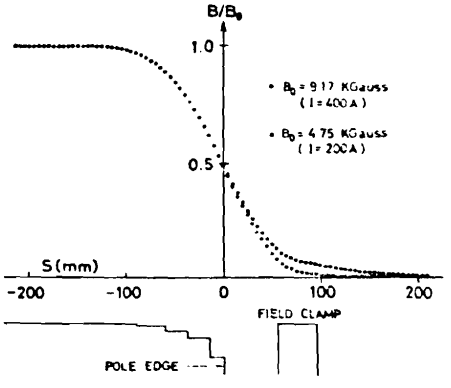

Fig.6 The distribution of the magnetic field along the beam orbit near the pole edge of the bending magnet. The effective edge was calculated according to these curves.

which extended to its tangential line at both sides. The mechanical pole edge was cut so as to enlarge the flat region of the effective focusing strength.[5)]

The field gradient of the quadrupole magnet was measured with twin coils translated horizontally and the induced voltage at each coil was fed into a VFC circuit of high sensitivity.[6)] The deviation of the field gradient along the radial direction was found to be less than 0.5 % in a whole region from x = - 85 to + 85 mm, where x denotes the distance from the central axis of the magnet as shown in Fig.7. The deviation of the effective length was also measured by the longer twin coils and was found to be less than 1% over the above region. The effective length was calculated to be 260 mm, while the geometrical one is 200 mm.

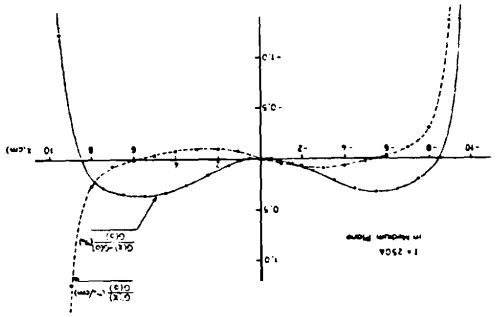

Fig.7 The field gradients of the quadrupole magnet (——), and the sextupole component (---) along the beam orbit. The value of G(0) is 0.44 kG/cm.

3.2. Multiturn Injection and RF Stacking

A combination of multiturn injection and RF stacking,[7,8)] is applied to the TARN. In this injection method, heavy ions from the cyclotron are injected into a transverse phase space via a magnetic and electrostatic inflectors while two bump magnets in the ring are excited, and then, are stacked into a longitudinal phase space by an RF field. This injection scheme is very efficient for obtaining higher beam intensity.

For the multiturn injection scheme, two bump magnets are located upstream and downstream from the injecting position. These magnets produce a distortion in the closed orbit between them and the distance between the magnets should be half a betatron wave-length in order to avoid any effect on other parts of the equilibrium orbit. The collapsing rate of the closed orbit distortion is determined so as to optimize the beam intensity stacked in the transverse phase space.

The procedure of RF stacking in the TARN is similar to the one which is used for the stacking of high energy proton beams at ISR, CERN.[9)]

The initial voltage of RF field is determined such that the separatrix well covers the phase space area of the injected beam, and is rather freely chosen within the limits of satisfying the above condition. Then the RF voltage for the capture process is determined at the same value as that during acceleration, 1100 V, at which the period of phase oscillation is 1.13 msec.

The rate of change of momentum for the synchronous particle, $\frac{dP/dt}{P}$, is designed at 1.52×10^{-2} (ms^{-1}) for the synchronous phase angle of 30° and RF voltage of 1100 V. The fractional momentum variation corresponding to the distance from the injection orbit to the bottom of the stacking orbit is 3.82 %. Then it takes 2.5 ms to change the momentum. The revolution-frequency difference between the injected beam and stacked one at the bottom is 32.6 kHz, and the corresponding RF frequency difference is 228 kHz.

During acceleration from the bottom to the top of the stacked region, the RF voltage is adiabatically reduced to the final voltage, 100 V. This reduction of RF voltage is necessary because the high RF voltage brings about undesirably large momentum spread of the stacked beam when the separatrix is moved to the top of the stacking orbit.

The momentum difference between the bottom and the top of the stacked beam is designed as 2.469 %, and hence the RF frequency must be changed by 149 kHz for this acceleration. In order to keep $\sin\phi_s = 0.5$ during the acceleration, the time derivative of the frequency must be 8.8 kHz/ms and the time required for the deposit is 17 ms.

Using the results of the above calculations, a total stacking number for both transverse and longitudinal phase spaces is obtained as a function of the half aperture offered for the multiturn injection. The total stacking number has the maximum value of about 1900 at $x_\beta = 20$ mm. The calculated envelopes of multiturn injected and RF stacked beams are shown in Fig. 8 as a function of length along the central orbit.

3.3 RF System, Beam Monitor and Control

The RF system is composed of a low level RF electronics system and high power parts including an accelerating cavity. The low level RF electronics plays an important role to obtain phase lock between

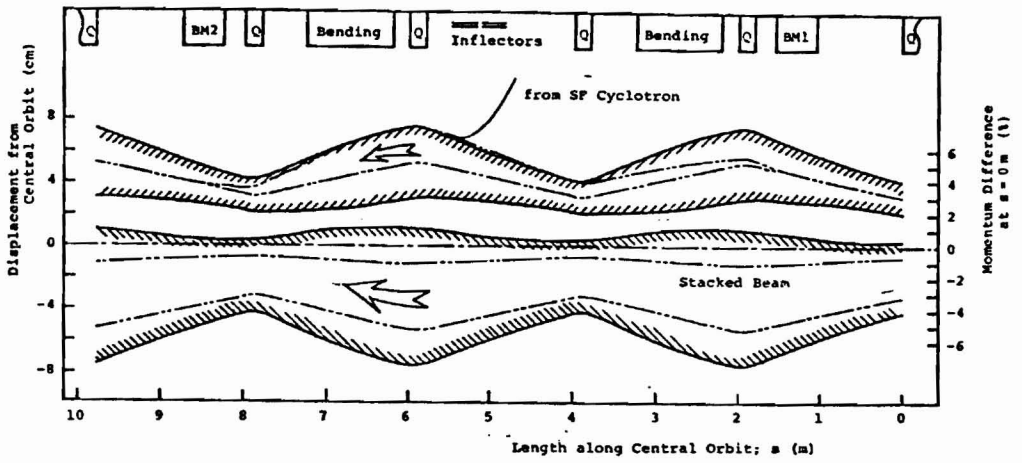

Fig.8 The envelopes of multiturn injected and RF stacked beams are shown by solid lines.

beam and RF accelerating field. Also it is used to control the accelerating voltage and frequency so as to obtain the optimum RF stacking condition. Programmed accelerating voltage and frequency are illustrated in Fig.9.

The amplitude of the RF field is modulated by a balanced modulator in accordance with the waveform from a function generator. The fast feedback voltage control function is given by an amplitude normalizer. It stabilizes the RF voltage against the variation of the cavity impedance due to the sweep of the frequency.

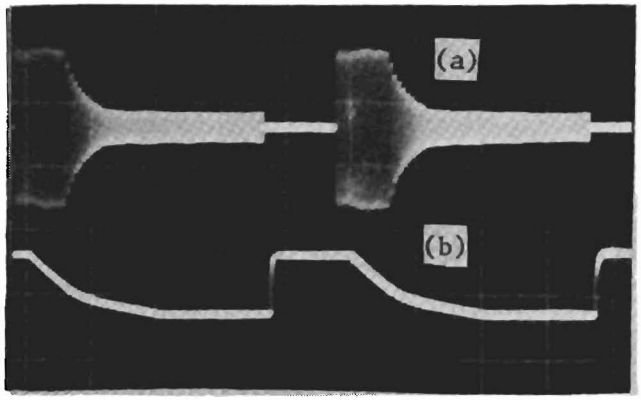

Fig.9 (a) Programmed accelerating voltage in the RF cavity. It rises from 0 V to 500 V and decreases to 100 V. (b) Accelerating frequency, which varies from the base frequency 8.00 MHz by 380 kHz. The time scale is 5 ms/div.

The phase difference between the accelerating field and the fundamental mode of the bunch signal is measured by a phase detector, where the beam phase information is derived from a core-type beam monitor with a resonator whose resonant frequency is adjusted at the RF frequency. The output signal of the phase detector is fed to a voltage controlled oscillator (VCO) through a summing amplifier. The

output frequency of the VCO is determined by the voltage on a varacter, which is composed of a program term from the function generator and a feedback one coming from the phase detector. The absolute value of the stable phase angle is determined by a phase shifter in the loop.

An accelerating structure is composed of two cavities with an electrical length of a quarter wave. In order to tune the cavity over an operating frequency and to reduce the size of the cavity, 24 ferrite rings, 328 mm O.D., 260 mm I.D. and 20 mm thick, are stacked in the cavity. Each ferrite ring is sandwiched by cooling copper discs. The resonant frequency of the cavity is varied by changing a capacitance between two inner conductors or by impressing the biasing magnetic field in the ferrite cores. The copper plate was wound around the ferrite rings by two-turns.

The RF power is fed to the cavity by a 5 kW RF power amplifier through a wide band transformer of a transmission type for matching their impedances. The transformer was also used to obtain two RF fields, whose phases are different by 180° from each other for the push-pull operation of the cavity.

Several kinds of beam monitors were prepared for efficient beam handling during injection and stacking. Electrostatic monitors with capacitive pickups and magnetic monitors using ferrite cores were used in a non-destructive manner, which is necessary for beam stacking. The former detects beam position by measuring asymmetry of induced charges on two electrodes. The magnetic monitor, where a coil picks up magnetic flux induced in the ferrite core, provides informations on beam intensity and phase. Output signals are converted into sine-wave through a tank circuit and fed to the RF control system. Four beam-dumping (Faraday-cup type) monitors are installed in the ring for studying the injection orbit of the beam in the ring. This detector, with sixteen strips of Be-Cu foil 500 μm in thickness and 2 mm in width, measures intensity and position simultaneously.

3.4. Vacuum System

On-beam pressure lower than 1×10^{-10} torr (1.33×10^{-8} Pa) is required to achieve 90 % survival probability of accumulated ions during a

period of 1 sec.[10] Since 1976, some preliminary tests on ultra-high vacuum (UHV) system have been carried out, two test stands for UHV studies being constructed. The vacuum chamber of test stand I is cylindrical, 30 cm in diameter and 200 cm in length, and is made of stainless steel 316L. The pumping system is composed of a 1500 ℓ/s titanium sublimation pump with liquid nitrogen shroud, and a 500 ℓ/s turbomolecular pump backed by a 400 ℓ/s oil diffusion pump. On the other hand, the vacuum chamber of test stand II is a prototype model of the bending section and the short straight section in the TARN. The pumping system is composed of a 400 ℓ/s sputter-ion pump and a 200 ℓ/s turbomolecular pump backed by a 100 ℓ/s turbomolecular pump. The baking and discharge cleaning effects were measured using test stands I and II, respectively.

Pumping characteristics have been studied to establish efficient procedures for baking out the vacuum chamber and glow discharge cleaning in Ar or Ar + O_2. It is found that the partial pressure of H_2O decreases significantly after glow discharge processing. In the typical spectrum, a peak at m/e = 16 was the highest one. It may be understood that this peak is not due to ions in gas-phase, but to O^+ ions emitted from the surface of the quadrupole mass-filter caused by electron impact desorption effect.[11] This peak is a very useful indicator of "cleanliness" of the surface in the system.

In November 1978, the whole vacuum system was assembled tentatively prior to installation into the magnet gaps. The system was baked at 250°C for 50 hours, and the average pressure of 2×10^{-11} torr was attained after 1,000 hour pumping down without glow discharge processing.

The system is illustrated in Fig. 10. The chamber has a circumferencial length of 31.8 m, and is divided into eight unit sections, each of which consists of one dipole magnet chamber of 45×234 mm^2 rectangular cross section, two quadrupole magnet chambers of 90×190 mm^2 diamond-shaped cross section, and a straight section chamber. These chambers are made of stainless steel 316L. Each pumping system is composed of a sputter-ion pump, a titanium sublimation pump, and a distributed pump, which is installed along the inside of the outer wall of the dipole magnet chamber and is also used as a high-voltage electrode for in situ glow discharge cleaning.[13]

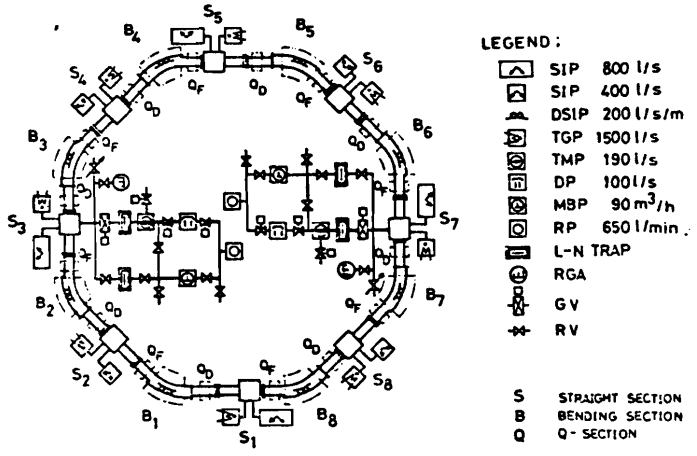

Fig.10 Vacuum System of the TARN

As shown in Fig.10, two roughing and auxiliary pumping systems are located at the straight sections S-3 and S-7, each of which comprises a turbomolecular pump backed by either an oil diffusion pump or a mechanical booster pump, and a rotary pump.

The straight section S-1 is connected to the injection beam transport line through three stages of differential pumping system.

3.5. Preliminary Results of Injection Test into TARN

The first trial of beam injection from the SF-Cyclotron to the TARN was performed successfully in August, 1979. The molecular hydrogen beam (H_2^+) of 14 MeV was used, because the dissociation cross section is similar to the charge exchange cross sections of heavy ions with residual gas molecules. In October, α particles (He^{2+}) of 28 MeV were also stacked in the ring.

Typical results of beam injection and accumulation using an electrostatic beam monitor are shown in the following figures. Figure 11 shows the 80μs long injected beams, which are pulse shaped from the C.W. cyclotron beam by a kicker magnet installed at an upstream position in the beam transport line. The upper picture shows the intensity of a single turn injected beam and the lower one shows the intensity of the beam four-turn injected when ν_x was adjusted to 2.25. According to the field decrease of the bump magnets, the beam is injected in multiturn fashion the intensity grows as illustrated in Fig. 12. The lower two curves show the current forms of the kicker and bump magnets. Accumulated intensity by multiturn injection is $\sim 10^8$ particles. The beam injected in multiturn is captured by the RF field. Fig.13 shows that the captured beam lasts till the next injection time after 25 ms. This

(b)

Fig.11 Shape of the injected beam with a length of 80 μs, a) single turn injection, b) four turn injection, observed by electrostatic beam monitor, 40 μs/div.

picture is taken by observing the 4th harmonics of the beam signals, avoiding severe noise from the RF source. Captured beam is moved to the stacking orbit by sweeping the RF frequency. The spectrum analyzer device is used for observing the beams, which have frequency components corresponding to the range of momentum spread of the beam. A typical result is shown in Fig.14. It is, however, difficult to estimate the intensity of stacked beam correctly at present. Further investigations for measuring the intensity of the stacked beam is needed. A sextupole magnet correction system for control of chromaticity is being designed in order to surmount the transverse coherent resistive wall instability. The intensity limit of the stable

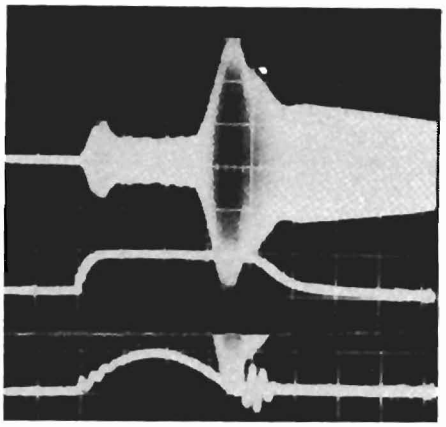

Fig.12 Injected beam in multi-turn (a), current form of kicker magnet (b), current form of bump magnets (c), 20 μs/div.

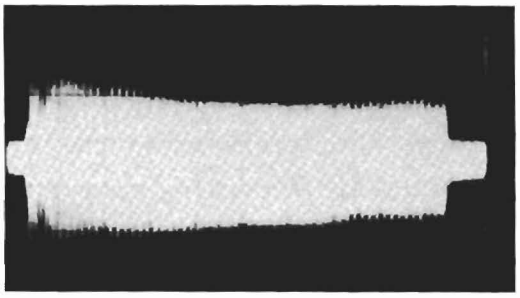

Fig.13 Captured beam by RF field, 2 ms/div, 4th harmonic observation of electrostatic monitor signal.

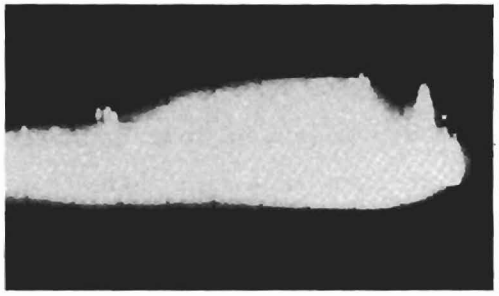

Fig.14 Display of spectrum analyser, illustrating the momentum spread of captured beam by the frequency sweep of 380 kHz.

beam is estimated at 6×10^8 without correction and 4×10^9 with correction for N^{5+}. The growth rate of the instability if we store 2×10^{10} N^{5+} into the ring is estimated at 0.2 sec.[13)]

ACKNOWLEDGMENT

The study of the project is advanced by the NUMATRON group at INS. The authors would like to express their thanks to the members of the group and also to the members of the SF-Cyclotron group. They are also grateful to Professor K. Sugimoto and M. Sakai for their continuous encouragement and to Dr. A. Garren for his calculations of the sextupole correction system.

REFERENCES

(1) Y. Hirao et al., "NUMATRON, Part II", INS-NUMA-5, 1977.

(2) Y. Hirao, "NUMATRON Project", Proc. of the Int. Conf. on Nuclear Structure, P.594 (1977).

(3) T. Katayama and S. Yamada, "Injection Method of the NUMATRON", Proc. of the 2nd Symp. on Acc. Sci. and Tech., p.151 (1978).

(4) Y. Hirao et al., "The INS 176 cm Sector Focusing Cyclotron", Proc. 7th Int. Conf. on Cyclotrons and Their Applications, p.103 (1975).

(5) M. Kumada et al., "Wide Aperture Q Magnet with End Cut Shaping", Proc. of 2nd Symp. on Acc. Sci. and Tech., p.75 (1978).

(6) M. Kumada et al., "Flux Meter for Field Gradient with Pendulum", Proc. of 2nd Symp. on Acc. Sci. and Tech., p.75 (1978).

(7) E. Keil, "Stacking in Betatron Phase Space for the ISR", ISR-TH/67-10.

(8) S. Yamada and T. Katayama, "Injection and Accumulation Method in the TARN", INS-NUMA-12 (1979).

(9) For example W. Schnell, Proc. of Conf. on High Energy Acc., Dubna (1963).

(10) K. Chida et al., "Vacuum System of the Test Ring for the NUMATRON", Proc. of the 2nd Symp. on Acc. Sci. and Tech., p.34 (1978).

(11) P. A. Redhead, "Ion Desorption by Electron Bombardment; Relation to Total and Partial Pressure Measurement", J. Vac. Sci. Technol. Vol.7, No.1, 182 (1970).

(12) A. G. Mathewson, J. Kouptsidis and L. Hipp, Proc. 7th Int. Vac. Congr. and 3rd Int. Conf. Solid Surfaces, Vienna, 1977.

(13) A. Garren and A. Noda, "A Sextupole Magnet Correction System for TARN", INS-NUMA-14, (1979).